Supplementary Materials

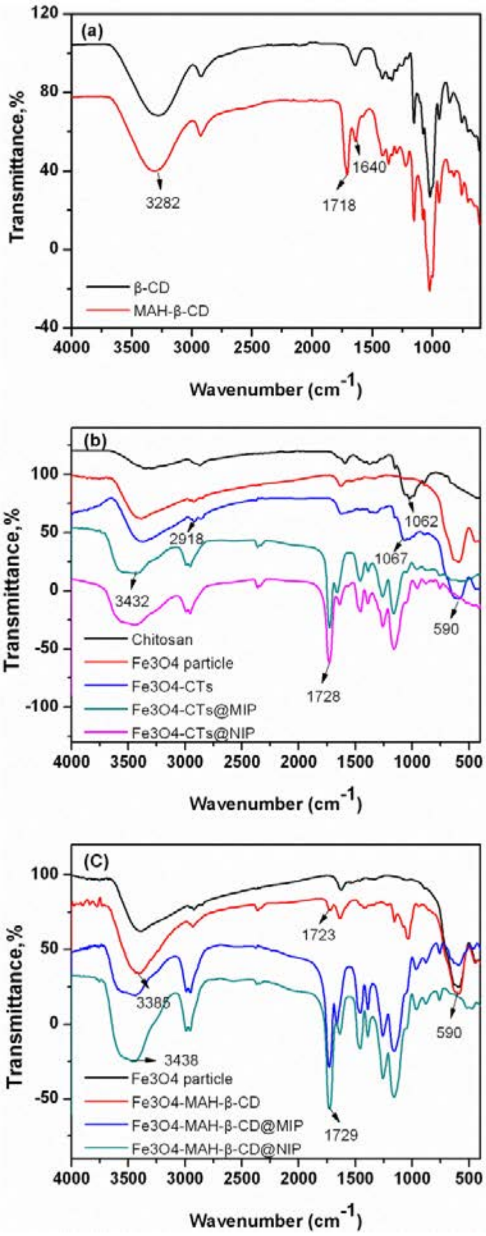

Figure S1. The FT-IR spectra of MAH-β-CD (**a**); Fe_3O_4-CTs@MIP and Fe_3O_4-CTs@NIP (**b**); Fe_3O_4-MAH-β-CD@MIP and Fe_3O_4-MAH-β-CD@NIP (**c**).

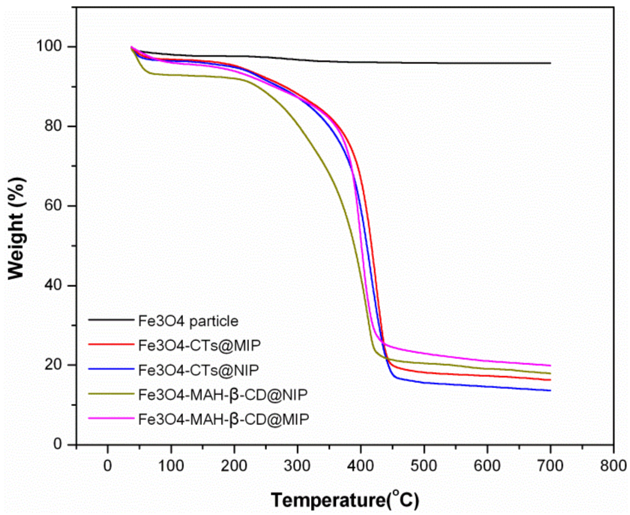

Figure S2. TGA curves of the Fe_3O_4 particle, Fe_3O_4-CTs@MIP, Fe_3O_4-CTs@NIP, Fe_3O_4-MAH-β-CD@MIP and Fe_3O_4-MAH-β-CD@NIP.

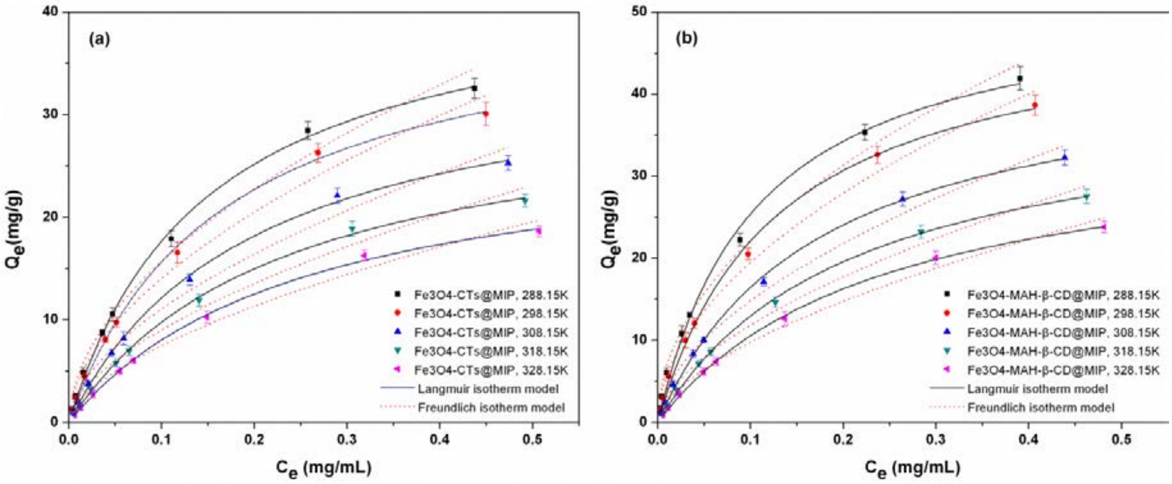

Figure S3. Adsorption isotherms of 2-aminopyridine binding onto Fe_3O_4-CTs@MIP (**a**) and Fe_3O_4-MAH-β-CD@MIP (**b**) at different temperatures.

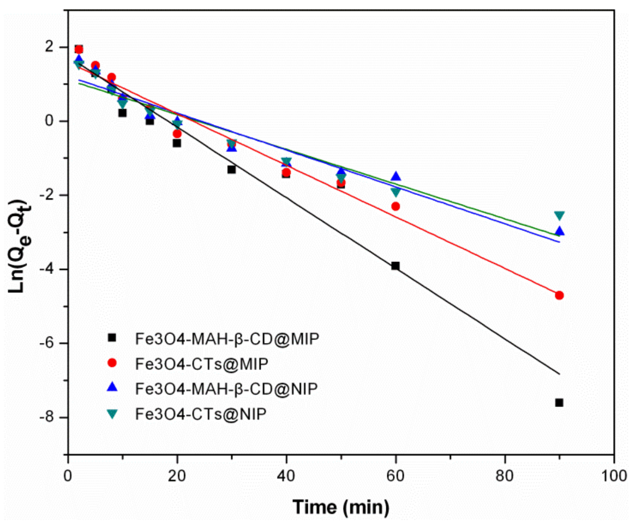

Figure S4. Pseudo-first-order kinetic model for the adsorption of 2-aminopyridine adsorption on Fe_3O_4-CTs@MIP, Fe_3O_4-CTs@NIP, Fe_3O_4-MAH-β-CD@MIP and Fe_3O_4-MAH-β-CD@NIP.

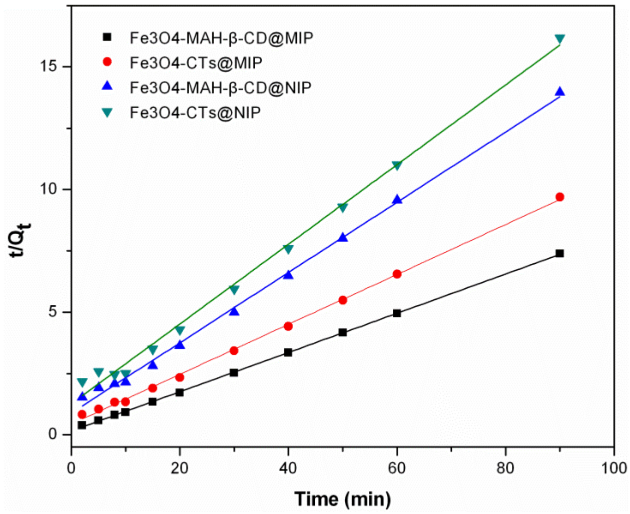

Figure S5. Pseudo-second-order kinetic model for the adsorption of 2-aminopyridine adsorption on Fe_3O_4-CTs@MIP, Fe_3O_4-CTs@NIP, Fe_3O_4-MAH-β-CD@MIP and Fe_3O_4-MAH-β-CD@NIP.

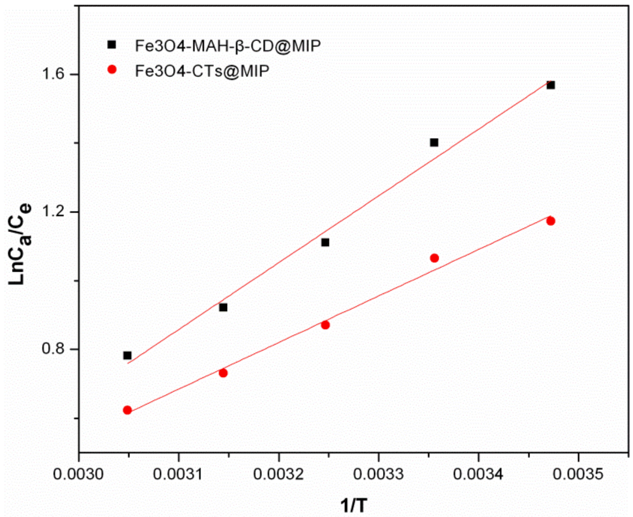

Figure S6. Van't Hoff plots of the uptake of 2-aminpyridine on Fe_3O_4-CTs@MIP and Fe_3O_4-MAH-β-CD@MIP.

Table S1. Kinetic parameters of the pseudo-first-order and pseudo-second-order rate equations for 2-aminopyridine adsorption on Fe_3O_4-CTs@MIP, Fe_3O_4-CTs@NIP, Fe_3O_4-MAH-β-CD@MIP and Fe_3O_4-MAH-β-CD@NIP (mean ± SD, *n*=3).

Polymer	Pseudo-First Order		R^2	Pseudo-Second Order		R^2
	k_1 (min^{-1})	$Q_{e,cal}$ ($mg{\cdot}g^{-1}$)		k_2 ($g{\cdot}mg^{-1}{\cdot}min^{-1}$)	$Q_{e,cal}$ ($mg{\cdot}g^{-1}$)	
Fe_3O_4-CTs@MIP	0.0696	4.93	0.9731	0.0239	9.83	0.9995
Fe_3O_4-CTs@NIP	0.0469	3.05	0.9252	0.0208	6.15	0.9945
Fe_3O_4-MAH-β-CD@MIP	0.0953	5.71	0.9460	0.0416	12.50	0.9997
Fe_3O_4-MAH-β-CD@NIP	0.0498	3.37	0.9375	0.0232	6.98	0.9971